

Phase locking of terahertz semiconductor dual-comb laser sources

Yiran Zhao^{1,2,6}, Ziping Li^{1,6}, Kang Zhou^{1,2,6}, Xiaoyu Liao^{1,2}, Wen Guan^{1,3}, Wenjian Wan¹, Sijia Yang^{1,2}, J. C. Cao^{1,2}, Dong Xu^{1,5}, Stefano Barbieri⁴, and Hua Li^{1,2*}

¹*Key Laboratory of Terahertz Solid State Technology, Shanghai Institute of Microsystem and Information Technology, Chinese Academy of Sciences, 865 Changning road, Shanghai 200050, China.*

²*Center of Materials Science and Optoelectronics Engineering, University of Chinese Academy of Sciences, Beijing 100049, China.*

³*School of Information Science and Technology, ShanghaiTech University, 393 Middle Huaxia Road, Shanghai 201210, China.*

⁴*Institute of Electronics, Microelectronics and Nanotechnology, University Lille, ISEN, CNRS, UMR 8520, 59652 Villeneuve d'Ascq, France.*

⁵*SIMIC Advanced Micro Semiconductors Co., Ltd., 888 2nd West Huanhu Street, Pudong, Shanghai 201306, China.*

⁶*These authors contributed equally: Yiran Zhao, Ziping Li, Kang Zhou.*

**Corresponding author. E-mail: hua.li@mail.sim.ac.cn.*

Dual-comb sources with equally spaced and low phase noise frequency lines are of great importance for high resolution spectroscopy and metrology. In the terahertz frequency regime, the electrically pumped semiconductor quantum cascade lasers (QCLs), demonstrating high output power, good far-field beam quality, and wide frequency coverage, are suitable candidates for frequency comb and dual-comb operations. Although free-running terahertz QCLs are able to work as frequency comb and dual-comb sources, the phase noises originated from the carrier and repetition frequencies' instabilities are relatively high, which strongly hinder the high precision applications. For a single laser frequency comb, the repetition frequency can be locked using a microwave injection locking and the carrier frequency can be locked

to a highly stable source. Although these techniques can be, in principle, applied to a dual-comb laser source, the complexity of simultaneous locking of four frequencies (two repetition frequencies and two carrier frequencies) makes it difficult to be implemented friendly. Here, we propose a method to lock a terahertz QCL dual-comb source by phase locking one of the dual-comb lines to a RF synthesizer. Without a need of locking of carrier offset and repetition frequencies of the two lasers, the technique can force one of the lasers to follow the “tone” of the other one. Although only one dual-comb line is locked, the phase noise of other dual-comb lines can be significantly reduced. Furthermore, we demonstrate that the dual-comb signal with the phase locked loop can generate periodic time pulses in a $2 \mu\text{s}$ time scale, which further indicates that the free running terahertz QCL comb can produce pulsed type waveforms without any active or passive mode locking techniques. The approach provides a convenient method to phase lock terahertz dual-comb sources, which can be further utilized for fast gas sensing and spectroscopy in terahertz regime.

A frequency comb^{1,2} consists of a series of coherent and equally spaced lines covering a broad spectrum. Frequency combs have revolutionized time and frequency metrology by exploiting their highly stable frequency lines and ultrafast optical pulses. Two frequencies can be used to fully describe a frequency comb, i.e., carrier offset frequency and repetition frequency. Once the two parameters are known, each line of a frequency comb can be accurately defined. Frequency combs can be straightforwardly used for high-precision spectroscopy by deploying a multiheterodyne dual-comb technique³ that consists of two frequency combs with slightly different repetition frequencies and the down-converted spectrum is recorded by mixing the two sets of modes onto a fast detector. In the last two decades, the frequency comb and dual-comb in near infrared and visible wavelengths have experienced significant developments targeting for various applications in spectroscopy, distance measurement, imaging, communications, and so on⁴⁻⁸.

Due to the importances of frequency comb and dual-comb sources in fundamental research and wide ranges of applications, ones have been dedicating to develop combs working at other wavelengths spanning the entire electromagnetic spectrum. Among it, the terahertz wave (0.1-10 THz) that is located between the microwave and infrared light has attracted more and more interests due to its potential applications in communications, security, health science, environmental monitoring, etc^{9,10}. Since the efficient terahertz radiation sources are lack, the frequency comb and dual-comb sources directly emitting in the terahertz frequency range have long remained nonexistent.

The indirect approach for generating terahertz frequency combs is to down-convert near-infrared frequency combs by nonlinear frequency conversion using photomixing in photoconductive antennas or optical rectification in nonlinear crystals^{11,12}. However, these down-conversion techniques require an external femtosecond laser pump, which results in a bulky terahertz comb system with weak optical power.

The semiconductor-based terahertz quantum cascade laser (QCL)¹³, showing high output power¹⁴, wide frequency coverage^{15,16}, high far-field beam quality¹⁷, is an ideal candidate for directly generating frequency comb and dual-comb operations in terahertz regime. Due to the fact that QCLs are electrically pumped, QCL frequency combs can offer the lowest size, weight and power (SWAP)¹⁸, which can allow these comb sources to be used for compact spectroscopy, imaging, and on-chip communications, etc. The simplest way to generate comb operation in a free running terahertz QCL is to exploit the four-wave mixing of the nonlinear QCL gain medium as well as the delicate group velocity dispersion engineering^{19–22}. Although the frequency comb operation can be achieved in a free running terahertz QCL, no experiment shows that it is able to produce optical pulses. Further coherence improvements of a single QCL comb can be implemented by locking the repetition frequency and carrier offset frequency, respectively, by using a microwave injection technique or a saturable absorber^{23–27}, and a phase locking with a highly stable femtosecond laser²⁸. These terahertz QCL combs with active or passive stabilization tools can produce short optical pulses between 1 and 16 ps^{27–32}. Concerning the dual-comb operation, up to now most terahertz QCL dual-comb sources are operated fully in free running without any control of repetition and/or carrier offset frequencies^{33–37}. In principle, the previously mentioned stabilization techniques can be applied to a dual-comb laser source. But four frequencies (two different repetition frequencies and two different carrier offset frequencies) should be locked simultaneously, which are too complicated to be implemented in a dual-comb source.

In this work, we report a phase locking of a terahertz QCL dual-comb source emitting around 4.2 THz. By down-converting one of the dual-comb lines to the working bandwidth of a phase locked loop (PLL), the dual-comb lines can be successfully locked. Note that the two terahertz QCLs are still operated in free running mode and only one dual-comb line is locked using the PLL. Experimental results indicate that the frequency stabilities of all dual-comb lines are significantly improved. The locked line at 90 MHz demonstrates a signal to noise ratio of 42 dB measured with a resolution bandwidth (RBW) of 1 Hz. Furthermore, we experimentally reveal that the phase locked dual-comb signal can generate periodic pulse trains in time domain. Because the down-converted dual-comb signal possesses the information of repetition and carrier offset frequencies

of each single frequency comb, the measured dual-comb signal can partially reflect the properties of single comb laser. Although the dual-comb time trace doesn't provide the output waveform of one single QCL comb, our result indicates a clear time periodicity with a pulsed type behaviour. The demonstration of phase locking of terahertz QCL dual-comb sources is an important step towards the development of high spectral resolution and high speed terahertz spectrometers and imagers.

Figure 1a shows the experimental setup of the phase locking of the terahertz dual-comb source. The inter-mode beatnote and multiheterodyne dual-comb signals in the radio frequency (RF) range are measured via Comb2 employing a laser self-detection scheme³⁶ (see Methods). In this experiment, only one of the dual-comb lines is finally selected and amplified for the phase locking (see Methods). The terahertz QCLs used in this work are based on a hybrid active region design (bound-to-continuum transitions for photon emission and fast longitudinal optical phonon scattering for depopulation in the lower laser state)^{38–40}, which has been experimentally proved to be suitable for frequency comb and dual-comb operations at frequencies around 4.2 THz^{21,27}. The nominal cavity length and ridge width for both laser combs are 5.5 mm and 150 μ m, respectively. However, due to the imperfections in the material growth and cleaving processes, the refractive index and the cavity length are not exactly identical for both combs which finally result in a slight difference in the inter-mode beatnote frequencies, i.e., f_{b1} and f_{b2} . This frequency difference is crucial for the dual-comb generation. As shown in Figure 1b, the spacing of the dual-comb spectra is equal to the difference between f_{b1} and f_{b2} . If the two inter-mode beatnote frequencies are identical, no dual-comb spectrum can be observed. In the optical frequency regime, one terahertz mode of Comb1 can beat with different modes of Comb2, so the dual-comb spectra can be generated at different carrier offset frequencies³⁶. In Figure 1b, we schematically show two dual-comb spectra at the first and second lowest offset frequencies (gray and green lines) below the inter-mode beatnote frequencies.

For the locking of dual-comb source, we actually just select one dual-comb line schematically marked by the circle in Figure 1b for the phase locking. The entire dual-comb spectrum will be first down-converted to lower frequencies around 90 MHz by beating with a microwave signal (red line) that is 90 MHz away from the selected dual-comb line. Then, the line at 90 MHz will be selected using a bandpass filter with a bandwidth of 5-10 MHz. Once the phase locked loop is switched on, the line will be locked by dynamically controlling the drive current of Comb2. It is worth noting neither the carrier offset frequencies nor the repetition frequencies of Comb1 and Comb2 are locked in this study. The PLL forces Comb2 to follow the behaviour of Comb1 and keep

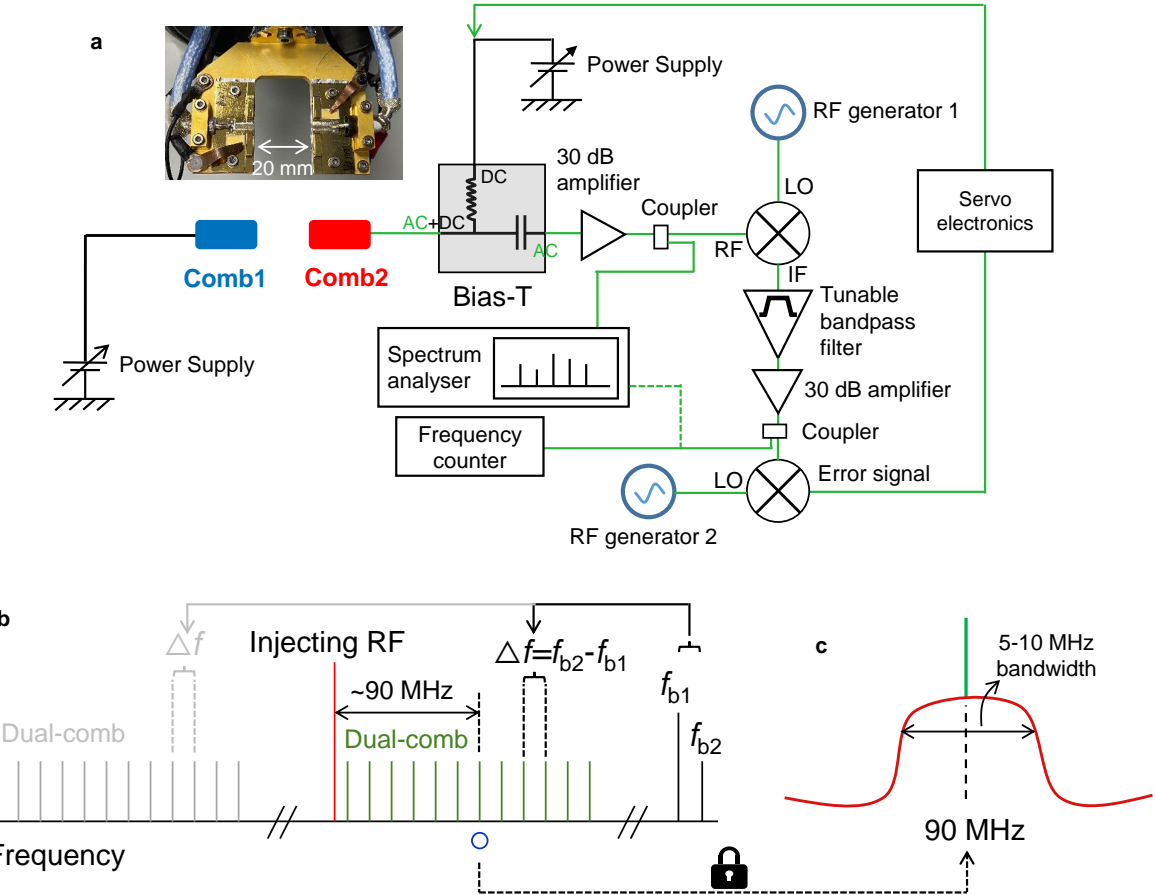


Figure 1: Experimental setup and frequency synthesis of phase locking of the terahertz dual-comb laser source. a, Experimental setup. Comb1 and Comb2 are single plasmon terahertz QCLs with a ridge width of $150 \mu\text{m}$ and a cavity length of 5.5 mm . RF generator 1 is used to mix the multiheterodyne dual-comb signal down to 90 MHz within the bandwidth of the PLL. RF generator 2 acts as a local oscillator (LO) to beat with the down-converted dual-comb line for generating the error signal to dynamically control the drive current of Comb2. Green lines represent high speed microwave cables and back lines are Bayonet Neil Concelman (BNC) cables. The inset is a photo of the dual-comb lasers mounted on a cold finger and the distance between the two laser front facets is 20 mm . IF: intermediate frequency. b, Frequency synthesis of the dual-comb phase locking experiment. f_{b1} and f_{b2} are the inter-mode beatnote frequencies of Comb1 and Comb2, respectively. Δf is the difference between f_{b1} and f_{b2} . c, Schematic plot of the phase locked down-converted dual-comb line at 90 MHz .

the dual-comb beating as a constant (see Supplementary Video 1 for a schematic demonstration of the moving of the terahertz modes without and with PLL). Although only one dual-comb line is

locked using the PLL, we find that other dual-comb lines are also much more stable compared to the lines without PLL (see Figure 4).

The measured light-current-voltage curves of Comb1 and Comb2 are shown in Figure 2a in continuous wave (cw) mode at a stabilized heat sink temperature of 32 K. Overall, the two lasers

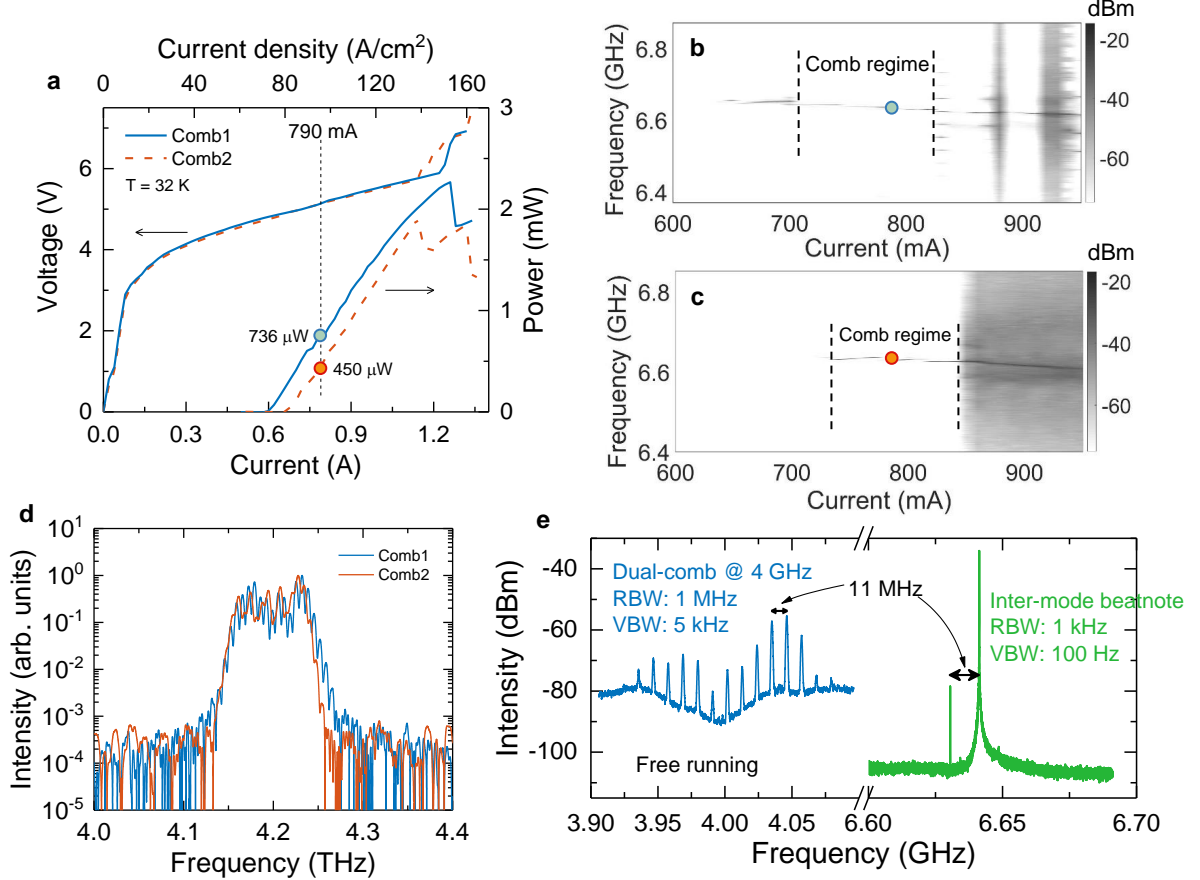


Figure 2: Laser performances and comb characteristics of both lasers with a cavity length of 5.5 mm and a ridge width of 150 μm . a, Light-current-voltage characteristics of the two QCLs measured in continuous wave (cw) mode. The vertical dashed line indicates the drive current of 790 mA which is set for the dual-comb operations for both lasers. b, c, Inter-mode beatnote maps of Comb1 and Comb2, respectively, measured with a RBW of 1 kHz and a video bandwidth (VBW) of 1 kHz. The current step is 10 mA. d, Normalized terahertz emission spectra of Comb1 and Comb2 measured at a drive current of 790 mA. e, Inter-mode beatnote and dual-comb spectra at 4 GHz measured from the laser dual-comb source. For all measurements, the temperature is stabilized at 32 K.

show uniform electrical and optical characteristics. The measured maximum output powers for the two lasers are slightly different, i.e., 2.2 mW for Comb1 and 1.9 mW for Comb2. This small difference is due to the nonuniform material growth, imperfect fabrication and device mounting processes. Figures 2b and 2c show the inter-mode beatnote maps for Comb1 and Comb2, respectively. We can see that as the current is higher than 850 mA, both lasers cannot work as ideal frequency combs since the inter-mode beatnote measured in this current range is either broad or multi-line structured. To obtain stable frequency comb operations for both lasers, we operate the two lasers at a drive current around 790 mA as marked in Figures 2a, 2b, and 2c. It is worth noting that the device dimensions, i.e., ridge width, cavity length, substrate thickness, etc., can influence the group velocity dispersions and finally affect the comb operation of the lasers. In Supplementary Figure S1, inter-mode beat note maps of two other lasers with different cavity lengths, i.e., 5 and 6 mm, and identical ridge width (150 μ m) and substrate thickness (100 μ m), are shown for comparison. It can be seen that the cavity length of 5.5 mm is optimal for comb operation. The emission spectra of the two lasers operated at 790 mA were measured using a Fourier transform infrared spectrometer with a spectral resolution of 0.1 cm^{-1} . As shown in Figure 2d, the two lasers show almost identical emission spectra. The strong spectral overlap is ideal for the dual-comb operation, which means that the spectral resource is not “wasted” during the multiheterodyne process. In Figure 2e, we show the measured inter-mode beatnote and dual-comb spectra measured when the two lasers are operated at 790 mA and 32 K in free running. Two narrow inter-mode beatnotes around 6.64 GHz are clearly observed with a frequency difference of 11 MHz which determines the line spacing of the dual-comb spectra. The dual-comb spectrum shown in Figure 2d is centered around 4 GHz, while this central frequency can be tuned by drive current (see Supplementary Figure S2). From the measured laser output power and the device mounting geometry, we can estimate that the power that is finally coupled into the detector Comb2 for the multiheterodyne process is around 140 nW³⁶.

In this work, we lock one of the dual-comb lines to a stable LO signal, which is made possible by sending the error signal back to dynamically control the drive current of Comb2 (see Figure 1a and Methods for the details of the PLL). The consequence of the phase locking technique is to electrically force Comb2 to follow the behaviour of Comb1 and keep the beating frequency of the two combs a constant (see Supplementary Video 1). Figure 3a shows the dual-comb spectrum measured when one of the dual-comb lines at 4.02 GHz (marked by a red arrow) is phase locked. The strong signal at 3.9281 GHz is the injecting RF signal which mixes the dual-comb signal down to 90 MHz. Then one of the down-converted dual-comb lines can be selected for phase locking. The spectrum of the locked line at 91.7079984 MHz is shown in Figure 3b. The flat pedestal from

89.4 to 93.8 MHz shows the bandwidth of the bandpass filter. The inset is the high resolution spectrum of the signal measured using a RBW of 1 Hz. It can be clearly seen that the line is phase locked and the signal to noise ratio (SNR) is measured to be greater than 40 dB. In Supplementary Video 2, the phase locking process is recorded, from which the line behaviour with and without PLL can be clearly observed. The simultaneous error signal with time that is sent to the Servo electronics for phase locking is also recorded as shown in Supplementary Video 3. Although the phase locking of the dual-comb line is achieved as shown in Figure 3b and Supplementary Video 2, the measured SNR of 42 dB at 1 Hz RBW is still far away from the optimal condition because the SNR doesn't scale with RBW, which indicates that the dual-comb line is partially phase locked.

To further quantify the frequency stability of the phase locked lines, we perform the frequency Allan deviation analysis and phase noise measurement. In Figure 3c, we plot the frequency Allan deviation as a function of integration time. To obtain the Allan deviation plot, the frequencies were recorded using a frequency counter with various gate times (see Figure 1a and Methods). For a clear comparison, the Allan deviation of the line at 90 MHz without PLL is also plotted as a black solid curve. One can see that the frequency stability is significantly improved once the phase locking is switched on. At short integration time around 1 millisecond, the calculated Allan deviation of the phase locked line is 6×10^{-4} , which is one order of magnitude lower than the value measured from the same line without PLL. More importantly, the results shown in Figure 3c indicate that the phase locking improves the long-term frequency stability. As the integration time is longer than 0.04 s, the Allan deviation of the non-phase-locked line starts to increase, while it continues to decrease with time for the phase locked line. At an integration time of 1 s, the phase locked line shows an Allan deviation of 2.5×10^{-5} which is almost two orders of magnitude lower than the line without PLL. In Supplementary Figure S3, we also show the Allan deviation of the amplitudes of dual-comb lines in different situations. Similar to the frequency Allan deviations shown in Figure 3c, the phase locked dual-comb line has a smaller amplitude Allan deviation than the dual-comb line without PLL.

Figure 3d plots the phase noise spectra for the dual-comb lines at 90 MHz with and without PLL. At a given frequency, the phase locked line always demonstrates lower phase noise than the dual-comb line without PLL. At 100 kHz and 1 MHz, the measured phase noises of the dual-comb line with PLL are -67 and -86 dBc/Hz, respectively. In Figure 3d, the phase noise spectrum of the inter-mode beatnote signal of Comb2 in free running is also plotted. It can be seen that the inter-mode beatnote signal shows much smaller phase noise than the dual-comb lines with and without PLL. It is measured that the phase noise is -106 dBc/Hz (-87 dBc/Hz) at 1 MHz (100

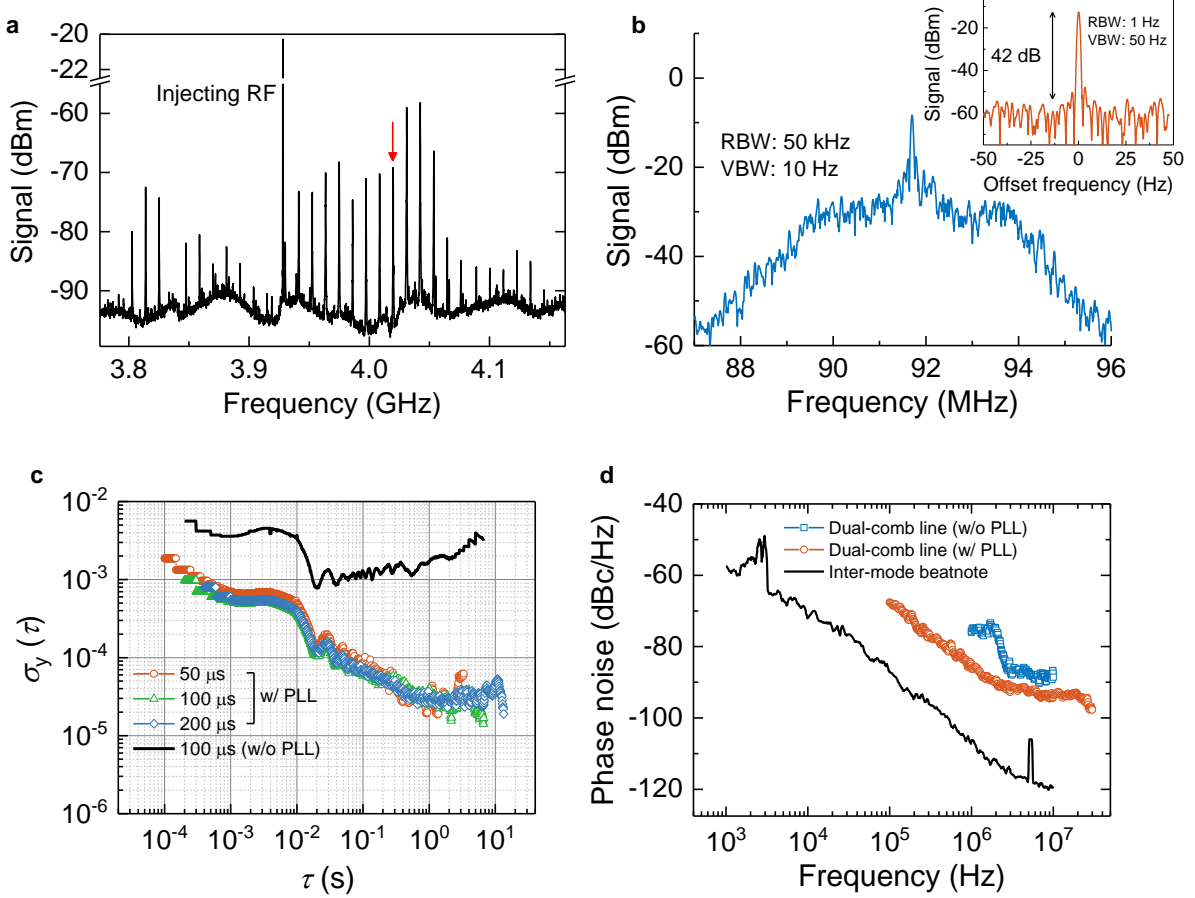


Figure 3: Phase locking of the terahertz dual-comb. a, Dual-comb spectrum around 4 GHz with one of the lines (indicated by the red arrow) phase locked to a stable RF synthesizer measured with a RBW of 100 kHz and a VBW of 500 Hz. The line with the highest power is the injecting RF that mixes the dual-comb line at 4.02 GHz (red arrow) down to 90 MHz located in the bandwidth of the bandpass filter for phase locking. b, Phase locked line at 91.7079984 MHz measured with a RBW of 50 kHz and a VBW of 10 kHz. The inset is the high resolution spectrum of the locked line measured with a RBW of 1 Hz. The offset frequency is subtracted by the central frequency of 91.7079984 MHz. c, Frequency Allan deviation plots measured using various gate times for the dual-comb line at 90 MHz with and without PLL. d, Phase noise spectra of the dual-comb line at 90 MHz with (circles) and without (squares) PLL. As a reference, the phase noise of the inter-mode beatnote signal at 6.64 GHz in free running is also shown as the solid line.

kHz) for the free running inter-mode beatnote signal at 6.64 GHz, which is even better than an integrated optoelectronic oscillator operating at 7-8 GHz⁴¹. The ultra-stable inter-mode beatnote finally contributes to the dual-comb operation and the phase locking of the dual-comb lines.

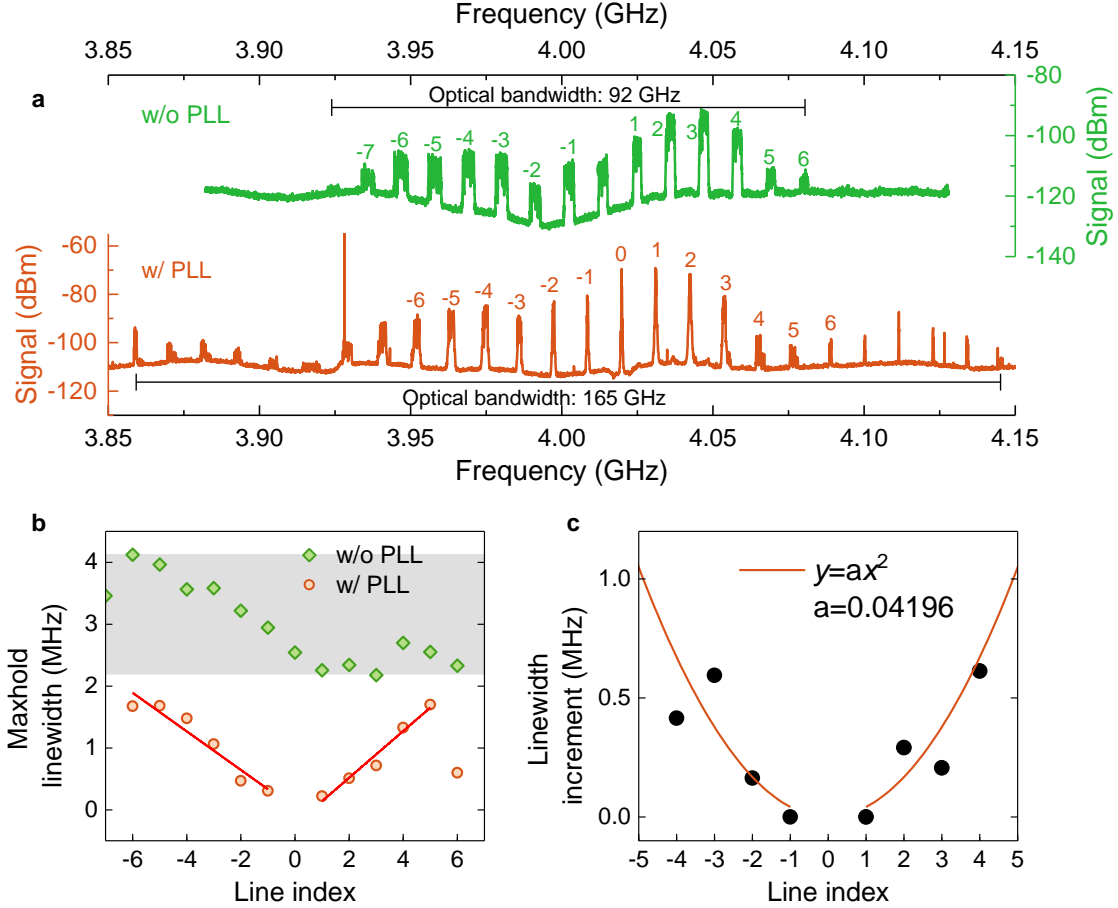


Figure 4: “Maxhold” measurement and linewidth comparison. a, Dual-comb spectra measured using the “maxhold” function of the spectrum analyser. The measurement duration for each “maxhold” trace is 30 seconds. The RBW and VBW parameters are set to 500 Hz and 50 Hz, respectively. b, Extracted “maxhold” linewidth as a function of line index for the dual-comb spectra without (green diamonds) and with (red circles) PLL. The line indices shown in b are identical as the ones shown in a. The red lines are only for a guide for the eyes. c, Linewidth increments for the closest 4 dual-comb lines with respect to the locked line extracted from b. The red curves in c show the calculated linewidth increment as a function of line index n . The function used for the calculation is $y=ax^2$ with the fitting parameter “a” being 0.04196.

To directly show the effect of the phase locking on the long-term frequency stability of the dual-comb spectra, in Figure 4a we plot the dual-comb traces without (green) and with (red) PLL acquired with a “maxhold” function of the spectrum analyser switched on for 30 seconds. We can clearly observe the significant improvement in long-term frequency stability for all the dual-comb lines once the phase locking is switched on. Furthermore, the number of dual-comb lines is

increased from 15 without PLL to 25 with PLL. The corresponding optical bandwidth is increased from 92 to 165 GHz as indicated in Figure 4a. The measured “maxhold” linewidths for the closest lines with respect to the phase locked line are plotted in Figure 4b. The line marked by “0” is the phase locked line. It can be clearly seen that as the lines are farther away from the phase locked line, the measured “maxhold” linewidths increase with the line index. The measured “maxhold” linewidths for the closest 6 dual-comb lines are smaller than 2 MHz with a smallest linewidth of 220 kHz for line 1. As a reference, the “maxhold” linewidths of the dual-comb lines without PLL extracted from the green curve of Figure 4a are also shown as diamonds in Figure 4b. As shown by the shaded area in Figure 4b, the “maxhold” linewidths for dual-comb lines without PLL spans in a range between 2.18 and 4.12 MHz. In Figure 4c, we plot the linewidth increment as a function of line index for the 4 closest dual-comb lines. As expected, due to the multiplication of the noise, a quadratic dependence of the linewidth increment on the line index is observed.

We also evaluate the time characteristics of the dual-comb signal. Figure 5a shows the experimental setup used for the time trace measurement of the dual-comb signal. Same as Figure 1a, the dual-comb signal is first down-converted to low frequencies around 90 MHz. Then, the signal is split into two using a microwave coupler, one is used for phase locking and the other one for time trace measurements. To obtain a clean signal for the time domain measurement, a low pass filter with a cutoff frequency of 200 MHz is used before the signal is sent to an oscilloscope. The filtered dual-comb signal is shown in Figure 5b where the line at 98 MHz is phase locked to a stable RF synthesizer. The time traces with and without PLL are shown in Figure 5c in a time scale of $2 \mu\text{s}$. It can be clearly seen that in the entire time domain, the dual-comb signal with PLL shows periodic pulse trains and each pulse can be well resolved in time. However, for the dual-comb signal without PLL, the pulses can be only observed in a limited time range of $1 \mu\text{s}$ and each pulse shows different pulse shape. As the time is far way from the center, no pulse can be observed. It is worth noting that the high peaks at the center of the horizontal axis (time=0 μs) are artificially introduced by the use of the low pass filter. As shown in Figure 5b, due to the use of the low pass filter, a step around 200 MHz is introduced into the spectrum, which then mathematically results in a strong peak at 0 position in the time trace after a Fourier transform. In Supplementary Figure S4, we show the comparison of time traces with and without the artificial central peaks, and the corresponding fast Fourier transform spectra. One can see that when the artificial peaks are removed, the Fourier spectrum doesn’t show the cutoff frequency step introduced by the low pass filter. Figure 5d plots the intensity of the time traces with and without PLL.

It is worth noting that the phase locking technique employed in this work is applied onto

the dual-comb signal to force one of the laser combs to follow the behaviour of the other laser. The target of the phase locking is to improve the frequency stability of the dual-comb operation. As shown in Figure 1a, the two lasers are still working in free running because we don't use any modulation and/or phase locking techniques to control the carrier offset and repetition frequencies of the two lasers. What we measured in Figure 5 is an electrical signal, but the signal also possesses the optical information translated from the terahertz, i.e., the carrier offset and repetition frequencies of the two free running QCL comb lasers. Although the dual-comb time trace shown

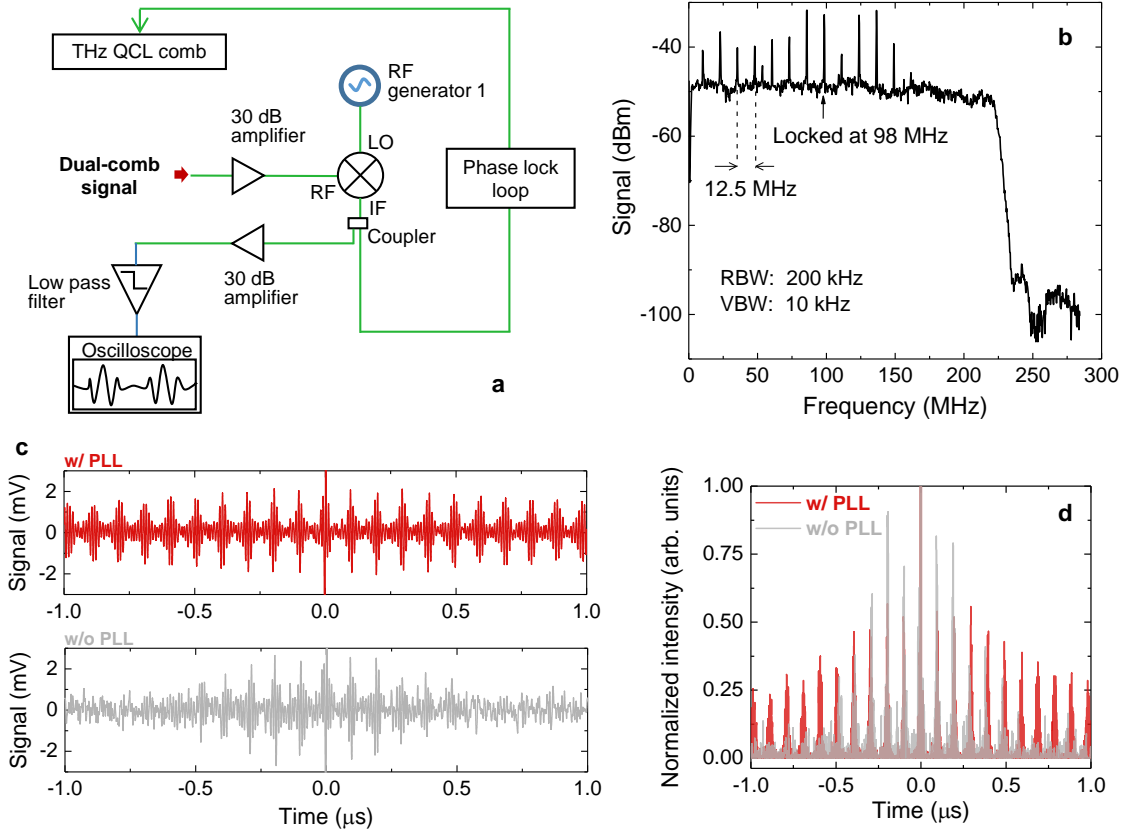


Figure 5: Time trace measurement of the terahertz dual-comb source. a, Experimental setup of the time trace measurement of the dual-comb signal. b, Down-converted dual-comb spectrum measured with a low pass filter with a cutoff frequency of 200 MHz. The dual-comb line at 98 MHz is phase locked. A RBW of 200 kHz and a VBW of 10 kHz were used for the dual-comb spectrum measurement. c, Measured time traces of the down-converted and filtered dual-comb signal with (upper panel) and without (lower panel) PLL. d, Normalized intensity plots of the data in c. All measurements are performed when QCL comb1 and comb2 are operated at 795 mA and 778 mA, respectively, at a stabilized temperature of 31 K.

in Figure 5c cannot provide the output waveform of one single QCL, our result indicates a clear time periodicity with a pulsed type behaviour. Actually, the technique is similar to the one reported in Ref. ²⁸ where a terahertz QCL comb was phase locked to an ultra-stable femtosecond laser and the comb lines were down-converted to low frequencies for time trace measurements. Here, in this work, we use the QCL comb itself as a “LO” for down-conversion. The two QCL combs beat with each other, due to the high frequency stability and strong coherence of the lasers, the comb lines can be also down-converted for time domain measurements. More importantly, in Ref. ²⁸ it is a must to apply the active mode locking onto a terahertz QCL to obtain stable pulses, while in this work we show that the free running terahertz QCL can emit pulsed type waveforms.

In summary, we have demonstrated the phase locking of a terahertz QCL dual-comb source emitting around 4.2 THz. By phase locking one of the down-converted dual-comb lines to a RF synthesizer, we are able to force one of the laser combs to follow the behaviour of the other comb, and finally significantly improve the frequency stability or coherence of all dual-comb lines. Experimental results reveal that the phase locked dual-comb lines show much better frequency/amplitude Allan deviations, phase noise, “maxhold” linewidths than the dual-comb lines without PLL. Furthermore, we experimentally show that the dual-comb signal with PLL can produce periodic time pulses. Since the dual-comb signal possesses the information of the carrier offset and repetition frequencies of both laser combs, the measured time trace of the dual-comb signal, in principle, indicates that the free running terahertz QCL comb is emitting pulsed type waveforms.

Methods

Terahertz QCL. The active region of the terahertz QCL used in this work is based on a hybrid design in which bound-to-continuum transitions are for generating terahertz photons and fast longitudinal optical phonon scatterings are for depopulation in the lower laser state. The QC structure is design for emitting photons at frequencies around 4.2 THz and the detailed layer structure can be found in ref. ⁴⁰. The QCL active region was grown using a molecular beam epitaxy system on a semi-insulating GaAs (100) substrate. The grown wafer was then fabricated into single plasmon waveguide geometry with a ridge width of 150 μm . To improve the thermal management, the laser substrate was thinned down to 100 μm using grinding and polishing techniques. Various cavity lengths (between 5 and 7 mm) were obtained by directly cleaving the fabricated laser ridges to form a Fabry-Perot resonator. We finally selected a cavity length of 5.5 mm in this work because it experimentally demonstrates optimal frequency comb operation (see Figure 2 and Supplementary Figure S1). For the laser dual-comb characterizations, two terahertz QCLs with identical cavity

length (5.5 mm) and ridge width (150 μm) were mounted onto a “Y” shape cold finger, see the inset of Figure 1a.

The cw output power of the terahertz QCLs were measured using a terahertz power meter (Ophir, 3A-P THz) and the lasers were operated in a constant current mode. To measure the power as accurately as possible, two off-axis parabolic mirrors were used for collecting and collimating the terahertz light into the power sensor. In addition, the beam path was purged with dry air to reduce the water absorption. The emission spectra shown in Figure 2c were measured with a Fourier transform infrared (FTIR) spectrometer (Bruker, v80) with a spectral resolution of 0.1 cm^{-1} (3 GHz).

Laser self-detection. Because the carrier inter-subband transitions in QCLs are fast processes in a time scale of picoseconds level, the QCL itself is capable for fast responding terahertz light⁴². When the modulated terahertz light is incident onto a QCL detector, the population inversion will be modulated by the optical light which results in the current modulation. This current change in the QCL device can then be measured directly using a spectrum analyser. In view of this, for the RF measurement in this work, the QCL can be inherently used as a fast detector as well as a terahertz emitter^{24,33,36,43}. Both the inter-mode beat note and down-converted dual-comb spectra can be measured simultaneously employing the laser self-detection scheme and registered by a spectrum analyser (Rohde & Schwarz, FSW26).

As shown in Figure 1a, in this experiment Comb2 is used as a fast detector. The detected heterodyne signal is sent to a Bias-T (Marki, BT2-0026) and then amplified for different measurements. To evaluate the long-term frequency drift, the “maxhold” measurement is used as shown in Figure 4a. When the “maxhold” function of the spectrum analyser is switched on, the spectral maxima at each sampling time are stored in a given measurement time duration.

Phase locked loop (PLL). The PLL has been already used for the repetition frequency locking of a single QCL comb and/or the locking of a QCL line to a stable source^{28,44,45}. Here, in this work we use the PLL to lock the terahertz QCL dual-comb lines. The experimental setup is shown in Figure 1a. Different from the repetition frequency locking of a single QCL comb where the inter-mode beatnote signal is sent to a phase lock loop, here one of the dual-comb lines is filtered out for the phase locking. In this work, the detected heterodyne signal is sent to Bias-T for measurement. The output of the AC port of the bias-T is a signal with different spectral information, including inter-mode beatnotes and their harmonics, dual-comb spectra at different carrier offset frequencies, and also the reflected signals from the RF generators (local oscillators). The signal is first amplified and mixed with the RF generator 1. To bring the signal down into the bandwidth of the PLL, the

frequency of RF generator 1 is fine tuned to finally obtain a series of dual-comb lines around 90 MHz. Then, a tunable bandpass filter with a bandwidth between 5-10 MHz is used to select just one dual-comb line. The selected line is amplified and sent to a mixer to beat with the signal from RF generator 2 (90 MHz). Finally, the error signal is sent to the Servo electronics to dynamically control the drive current of Comb2. For a stable locking, the power values of RF generator 1 and RF generator 2 are set to be 10 dBm and 0 dBm, respectively.

Allan deviation measurement. The frequency Allan deviations are measured using a frequency counter with a bandwidth of 350 MHz (Keysight, 53230 A). To accurately measure the single frequency signal, a filter with a bandwidth of 5-10 MHz is used to filter out other frequency components. The frequency counter is set to work in a continuous mode and the sampling rate is determined by setting the gate time parameter.

The recorded frequency values as a function of time can be used to calculate the Allan deviation for various integration time τ by following the equation

$$\sigma_y(\tau) = \left[\frac{1}{2M} \sum_{i=0}^{M-1} (y(i+1) - y(i))^2 \right]^{1/2} \quad (1)$$

where $M=T/\tau-1$ with T being the entire measurement interval, $y(i)=\frac{<\alpha(t_0+i\tau)>_\tau-\alpha_0}{\alpha_0}$ with $<\alpha(t_0+i\tau)>_\tau$ being the frequency averaged over a time interval τ and α_0 the mean value of the measured frequencies.

Time trace measurement. To obtain the time characteristics of the pure dual-comb signal, we first down-convert the dual-comb signal to lower frequencies and other frequency components are filtered out by using a low pass filter as shown in Figure 5a. The time traces shown in Figure 5c were measured using an oscilloscope with a bandwidth of 20 GHz (LeCroy SDA820Zi-B). Before the down-converted dual-comb signal was sent to the oscilloscope, it was first amplified by 30 dB to meet the power requirement for time trace measurements and then filtered using a low pass filter with a nominal cutoff frequency of 200 MHz. To facilitate the time trace measurements, the signal was triggered by itself and a large average number of 2048 was used.

Data availability. All data that support the findings of this study are available from the corresponding author on reasonable request.

Code availability. Custom codes are available from the corresponding author on reasonable request.

References

1. Holzwarth, R. *et al.* Optical frequency synthesizer for precision spectroscopy. *Physical Review Letters* **85**, 2264–2267 (2000).
2. Udem, T., Holzwarth, R. & Hänsch, T. W. Optical frequency metrology. *Nature* **416**, 233–237 (2002).
3. Keilmann, F., Gohle, C. & Holzwarth, R. Time-domain mid-infrared frequency-comb spectrometer. *Optics Letters* **29**, 1542–1544 (2004).
4. Villares, G., Hugi, A., Blaser, S. & Faist, J. Dual-comb spectroscopy based on quantum-cascade-laser frequency combs. *Nature Communications* **5**, 5192 (2014).
5. Coddington, I., Newbury, N. & Swann, W. Dual-comb spectroscopy. *Optica* **3**, 414–426 (2016).
6. Yan, M. *et al.* Mid-infrared dual-comb spectroscopy with electro-optic modulators. *Light: Science & Applications* **6**, e17076 (2017).
7. Kippenberg, T. J., Gaeta, A. L., Lipson, M. & Gorodetsky, M. L. Dissipative kerr solitons in optical microresonators. *Science* **361**, eaan8083 (2018).
8. Picque, N. & Hansch, T. W. Frequency comb spectroscopy. *Nature Photonics* **13**, 146–157 (2019).
9. Ferguson, B. & Zhang, X. C. Materials for terahertz science and technology. *Nature Materials* **1**, 26–33 (2002).
10. Tonouchi, M. Cutting-edge terahertz technology. *Nature Photonics* **1**, 97–105 (2007).
11. Finneran, I. A. *et al.* Decade-spanning high-precision terahertz frequency comb. *Physical Review Letters* **114**, 163902 (2015).
12. Yasui, T. *et al.* Adaptive sampling dual terahertz comb spectroscopy using dual free-running femtosecond lasers. *Scientific Reports* **5**, 10786 (2015).
13. Köhler, R. *et al.* Terahertz semiconductor-heterostructure laser. *Nature* **417**, 156–159 (2002).
14. Li, L. *et al.* Multi-watt high-power thz frequency quantum cascade lasers. *Electronics Letters* **53**, 799–800 (2017).

15. Rösch, M. *et al.* Heterogeneous terahertz quantum cascade lasers exceeding 1.9 thz spectral bandwidth and featuring dual comb operation. *Nanophotonics* **7**, 237–242 (2018).
16. Chan, C. W. I., Hu, Q. & Reno, J. L. Ground state terahertz quantum cascade lasers. *Applied Physics Letters* **101**, 151108 (2012).
17. Wan, W. J., Li, H. & Cao, J. C. Homogeneous spectral broadening of pulsed terahertz quantum cascade lasers by radio frequency modulation. *Optics Express* **26**, 980–989 (2018).
18. Fortier, T. & Baumann, E. 20 years of developments in optical frequency comb technology and applications. *Communications Physics* **2**, 153 (2019).
19. Burghoff, D. *et al.* Terahertz laser frequency combs. *Nature Photonics* **8**, 462–467 (2014).
20. Rösch, M., Scalari, G., Beck, M. & Faist, J. Octave-spanning semiconductor laser. *Nature Photonics* **9**, 42–47 (2015).
21. Zhou, K. *et al.* Ridge width effect on comb operation in terahertz quantum cascade lasers. *Applied Physics Letters* **114**, 191106 (2019).
22. Piccardo, M. *et al.* Frequency combs induced by phase turbulence. *Nature* **582**, 360–364 (2020).
23. Oustinov, D. *et al.* Phase seeding of a terahertz quantum cascade laser. *Nature Communications* **1**, 69 (2010).
24. Gellie, P. *et al.* Injection-locking of terahertz quantum cascade lasers up to 35GHz using rf amplitude modulation. *Optics Express* **18**, 20799–20816 (2010).
25. Forrer, A. *et al.* Photon-driven broadband emission and frequency comb RF injection locking in thz quantum cascade lasers. *ACS Photonics* **7**, 784–791 (2020).
26. Rodriguez, E. *et al.* Tunability of the free-spectral range by microwave injection into a mid-infrared quantum cascade laser. *Laser & Photonics Reviews* **14**, 1900389 (2020).
27. Li, H. *et al.* Graphene-coupled terahertz semiconductor lasers for enhanced passive frequency comb operation. *Advanced Science* **6**, 1900460 (2019).
28. Barbieri, S. *et al.* Coherent sampling of active mode-locked terahertz quantum cascade lasers and frequency synthesis. *Nature Photonics* **5**, 306–313 (2011).

29. Bachmann, D. *et al.* Short pulse generation and mode control of broadband terahertz quantum cascade lasers. *Optica* **3**, 1087–1094 (2016).
30. Mottaghizadeh, A. *et al.* 5-ps-long terahertz pulses from an active-mode-locked quantum cascade laser. *Optica* **4**, 168–171 (2017).
31. Wang, F. *et al.* Short terahertz pulse generation from a dispersion compensated modelocked semiconductor laser. *Laser & Photonics Reviews* **11**, 1700013 (2017).
32. Wang, F. H. *et al.* Ultrafast response of harmonic modelocked thz lasers. *Light: Science & Applications* **9**, 51 (2020).
33. Rösch, M. *et al.* On-chip, self-detected terahertz dual-comb source. *Applied Physics Letters* **108**, 171104 (2016).
34. Yang, Y. *et al.* Terahertz multiheterodyne spectroscopy using laser frequency combs. *Optica* **3**, 499–502 (2016).
35. Sterczewski, L. A. *et al.* Terahertz hyperspectral imaging with dual chip-scale combs. *Optica* **6**, 766–771 (2019).
36. Li, H. *et al.* Toward compact and real-time terahertz dual-comb spectroscopy employing a self-detection scheme. *ACS Photonics* **7**, 49–56 (2020).
37. Sterczewski, L. A. *et al.* Terahertz spectroscopy of gas mixtures with dual quantum cascade laser frequency combs. *ACS Photonics* **7**, 1082–1087 (2020).
38. Scalari, G., Hoyler, N., Giovannini, M. & Faist, J. Terahertz bound-to-continuum quantum-cascade lasers based on optical-phonon scattering extraction. *Applied Physics Letters* **86**, 181101 (2005).
39. Wienold, M. *et al.* Low-threshold terahertz quantum-cascade lasers based on GaAs/Al_{0.25}Ga_{0.75}As heterostructures. *Applied Physics Letters* **97**, 071113 (2010).
40. Wan, W., Li, H., Zhou, T. & Cao, J. Homogeneous spectral spanning of terahertz semiconductor lasers with radio frequency modulation. *Scientific Reports* **7**, 44109 (2017).
41. Tang, J. *et al.* Integrated optoelectronic oscillator. *Optics Express* **26**, 12257–12265 (2018).
42. Li, H. *et al.* Dynamics of ultra-broadband terahertz quantum cascade lasers for comb operation. *Optics Express* **23**, 33270–33294 (2015).

43. Li, Z. *et al.* On-chip dual-comb source based on terahertz quantum cascade lasers under microwave double injection. *Physical Review Applied* **12**, 044068 (2019).
44. Consolino, L. *et al.* Fully phase-stabilized quantum cascade laser frequency comb. *Nature Communications* **10**, 2938 (2019).
45. Cappelli, F. *et al.* Retrieval of phase relation and emission profile of quantum cascade laser frequency combs. *Nature Photonics* **13**, 562–568 (2019).

Acknowledgements This work is supported by the National Science Fund for Excellent Young Scholars (62022084), Shanghai Outstanding Academic Leaders Plan (20XD1424700), Shanghai Youth Top Talent Support Program, the National Natural Science Foundation of China (61875220, 61927813, 61404150, 61405233, and 61704181), the “From 0 to 1” Innovation Program of the Chinese Academy of Sciences (ZDBS-LY-JSC009), and the Major National Development Project of Scientific Instrument and Equipment (2017YFF0106302). The authors thank R. Qian and X. W. Sun for a loan of a RF synthesizer.

Author contributions H.L. conceived the study. Z.P.L., W.J.W., Y.R.Z., W.G., and S.J.Y. fabricated the terahertz QCLs and carried out the basic device measurement. Y.R.Z., Z.P.L., K.Z., X.Y.L., W.G., and H.L. performed dual-comb measurements. K.Z. and H.L. did the noise analysis. Y.R.Z., Z.P.L., X.Y.L., W.G., and H.L. performed the phase locking of the terahertz dual-comb source. H.L., S.B., Y.R.Z., Z.P.L., K.Z., J.C.C, and D.X. participated in the date analysis. H.L. wrote the manuscript with contributions from all other authors. H.L. supervised the project.

Addition information Correspondence and requests for materials should be addressed to H.L. (email: hua.li@mail.sim.ac.cn).

Competing financial Interests The authors declare that they have no competing financial interests.